Electronic Supplementary Information to:

How water desorbs from calcite

Tobias Dickbreder,*[1] Dirk Lautner,[2] Antonia Köhler,[1] Lea Klausfering,[1] Ralf Bechstein[1] and

Angelika Kühnle*[1]

[1] Faculty of Chemistry, Physical Chemistry I, Bielefeld University, 33615 Bielefeld, Germany.

[2] Institute of Physical Chemistry, Johannes Gutenberg University Mainz, Duesbergweg 10-14, 55099 Mainz, Germany.

MULTILAYER DESORPTION SIGNALS

Figure S1 shows experimental desorption curves with varying initial coverages of water desorbing from calcite (10.4). As explained in the main text, we used the integral over the observed α, β-double peak to determine the intensity corresponding to one monolayer and calibrate the measured desorption rates. To this end, we do not include desorption rates measured above 320 K in the calibration because of the baseline artifacts discussed in the main text. Moreover, for the desorption curves in Figure S1(a) we also exclude desorption rates measured below 200 K as the desorption curve used for calibration (blue line in Figure S1(a)) already contains a small second-layer desorption signal. In this case, an integration over the full desorption spectra would yield an erroneously high monolayer saturation. Moreover, we do not use the desorption curve with the next smaller α, β-peak intensity, because its total intensity is significantly smaller and, thus, the expected error is much higher than for the described procedure. Note that the discussed calibration of the desorption rate does not affect the shape of the desorption curves but only scales the displayed desorption rates. Desorption curves for very high initial coverages up to 6.0 ML are shown in Figure S1(b). The desorption curves show the development of three additional desorption peaks below 180 K, namely the γ peak at 163 K, the δ peak at 160 K and the ε peak at 153 K. We assign these to desorption of water molecules from the second and higher water layers as explained in the main text. The peak ε peak is the last peak we observe with increasing initial coverage and its peak temperature is in excellent agreement with the desorption temperatures reported in literature for multilayer water desorption from various substrates [1-3]. Consequently, we assign the ε peak to desorption of water molecules bound in the multilayer.
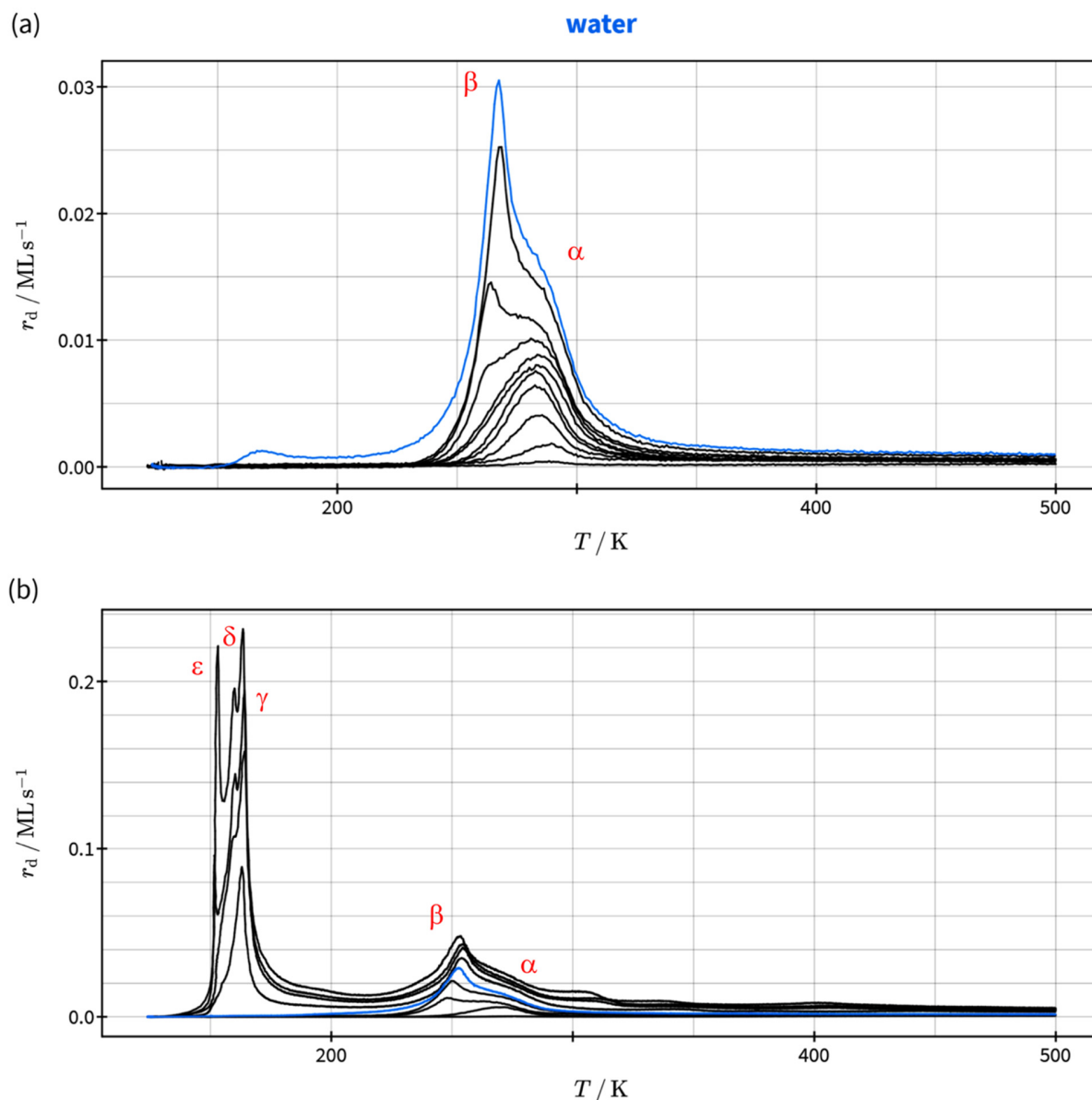
Figure S1. Experimental TPD curves of water desorbing from calcite (10.4) including desorption curves with initial coverages above 1.0 ML. (a) Set of desorption curves with initial coverages slightly above 1.0 ML showing the plateau area developing between 180 K and 230 K after saturation of the α, β-double peak. The desorption curves were measured in the temperature range from 120 K to 500 K. (b) Desorption curves showing the appearance of additional γ, δ and ε desorption peaks below 180 K for initial coverages up to 6.0 ML. The desorption curves were measured in the temperature range from 120 K to 600 K. In (a) and (b) one monolayer is defined by the integrated saturation intensity of the α, β-double peak between 200 K and 320 K. The desorption curves used for determination of the saturated peak intensity are highlighted in blue. All displayed desorption curves were recorded with a heating rate of 1 K s^{-1} at a mass-to-charge ratio of m/z 18.

Experimental desorption curves measured for different initial coverages of ethanol on calcite (10.4) are shown in Figure S2. As described for the desorption curves of water, the calibration factor for the desorption curves of ethanol is determined from the integral over the saturated monolayer desorption signal. Again, we excluded desorption rates measured above 350 K due to baseline artifacts. Here, we chose the desorption curve highlighted as a green line in Figure S2 for calibration, because the two desorption curves with higher monolayer peak intensities were measured for initial coverages significantly above one monolayer. This causes a baseline offset originating from the observed intensive multilayer desorption signal and, thus, the integrated peak intensity would be erroneously high.
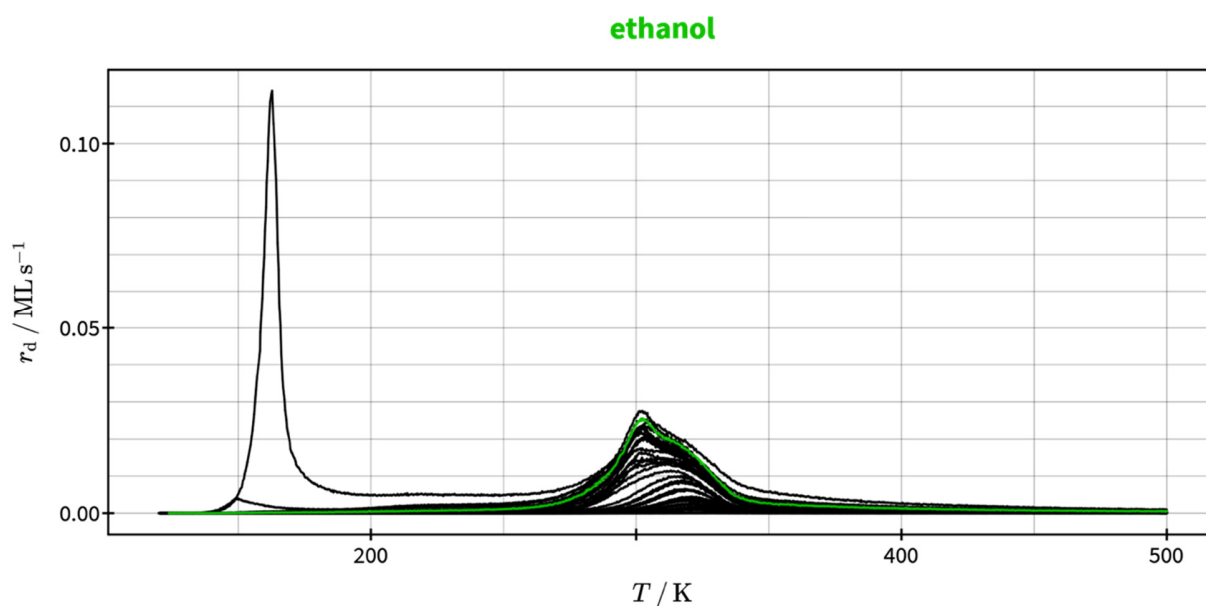

Figure S2. Experimental TPD curves of ethanol desorbing from calcite (10.4) including desorption curves with initial coverages above 1.0 ML, where the desorption curve corresponding to a coverage of 1.0 ML is highlighted in green. One monolayer (1.0 ML) is defined by the integrated saturation intensity of the observed double-peak structure. The curves were measured in the temperature range from 120 K to 500 K with a heating rate of 1 K s^{-1} at a mass-to-charge ratio of m/z 31.

TWO-SITE EXCHANGE MODEL

In the main text, we use a two-site-exchange model to elucidate whether the desorption curves of water and ethanol can be explained by a (2x1) reconstruction of the calcite surface. Here, we derive the relevant model equations and explain how we used these equations to simulate desorption curves.

4.1 Model Description

In our two-site-exchange model, the surface consists of N_{ad} well-defined adsorption sites. Each adsorption site is either of type A or type B and can be occupied only once. The site density ρ_A equals the fraction of type A sites in all adsorption sites and the coverage θ_A of type A is the fraction of occupied A sites with respect to all adsorption sites. The site density ρ_B and coverage θ_B for type B adsorption sites are defined accordingly. Since a (2x1) reconstructed surface has the same number of adsorption sites of type A and B, the site densities in our case are given by $\rho_A = \rho_B = 0.5$. In general, however, the presented model can be used for systems with other site densities as well.

In terms of processes, our model explicitly includes the exchange of molecules between adsorption sites of different types — *i.e.*, from A to B and from B to A — as well as desorption from both types of adsorption sites. Additionally, we implicitly consider diffusion between adsorption sites of the same type by assuming that all adsorption sites of the same type are occupied with equal probability (θ_A for type A sites and θ_B for type B sites).

To simulate desorption curves based on our model, we need to calculate the total normalized desorption rate[1] r_d as a function of temperature. For a system with two adsorption sites, this total desorption rate is the sum of the desorption rates from both types of adsorption sites. Here, we describe the desorption from sites A and B with a Polanyi-Wigner style approach, *i.e.,* the normalized desorption rate for one type of adsorption sites is given by $r_{d,i} = k_{d,i}\theta_i$ with i = A, B. Consequently, the total desorption rate is given by equation 1.

$$r_d = k_{d,A}\theta_A + k_{d,B}\theta_B \qquad (1)$$

As shown in equation 1, the total desorption rate depends on the rate constants for desorption from both sites as well as the coverages of sites A and B. To obtain the site coverages θ_A and θ_B, we need to consider the exchange of molecules between the adsorption sites. In our case, the proximity of the desorption temperatures of molecules adsorbed on site A and B (see Figure 2a) indicate that the energy difference between both types of adsorption sites is small compared to the desorption energy. Based on this observation, we expect that both exchange and diffusion are fast as compared to desorption. Consequently, we assume that the system is in equilibrium with respect to the occupation of different adsorption sites on the timescale of desorption. We can thus describe the exchange process by the corresponding equilibrium constant K_{AB}, instead of explicitly considering the exchange rates in both directions. The exchange can be described as a reaction of one occupied adsorption site A (coverage θ_A) with an unoccupied site B (coverage $\rho_B - \theta_B$) resulting in an unoccupied site A (coverage $1 - \rho_B - \theta_A$) and an occupied site B (coverage θ_B), and *vice versa.*

---

[1] The normalized desorption rate r_d is the desorption rate divided by the number of adsorption sites per layer N_{ad}.

As the equilibrium constant is given by the ratio of product and educt coverages, we obtain equation 2.

$$K_{\mathrm{AB}} = \frac{(1 - \rho_B - \theta_A)\theta_B}{(\rho_B - \theta_B)\theta_A} \qquad (2)$$

Additionally, the calculation of desorption curves requires a temperature-dependent description of the rate constants. To this end, we apply transition state theory according to equation 3, where x denotes the described process (e.g., $x =$ d for desorption) and the quantities ΔE_x and ΔS_x are the potential energy barrier and entropy change of the process respectively.

$$k_x = \frac{k_B T}{h} \exp\left(\frac{\Delta S_x}{k_B} - \frac{\Delta E_x}{k_B T}\right) \qquad (3)$$

To obtain the equilibrium constant of site exchange K_{AB} we make use of the fact that it can also be described by the ratio of the rate constants of exchange $k_{\mathrm{A \to B}}/k_{\mathrm{B \to A}}$. Thus, the applied transition state theory approach results in equation 4, which means that K_{AB} only depends on the potential energy and entropy differences between A and B ΔE_{AB} and ΔS_{AB} and not on the barriers of the exchange. As a consequence, our model depends on six independent kinetic parameters, *i.e.,* two parameters for each rate constant of desorption and two additional parameters to describe the equilibrium constant of site exchange. For the fit of our model to the experimental data and interpretation of the results, however, it is desirable to minimize the number of model parameters. In order to do so, we assume that the desorption from both types of adsorption sites is reversible with a negligible energy barrier as observed for many cases of molecular adsorption in literature [4]. This assumption enables us to express ΔE_{AB} and ΔS_{AB} by the kinetic parameters of desorption

and, thus, the potential energy barrier between A and B is given by $\Delta E_{AB} = \Delta E_{d,B} - \Delta E_{d,A}$ and the entropy difference by $\Delta S_{AB} = \Delta S_{d,B} - \Delta S_{d,A}$.

$$K_{AB} = \exp\left(\frac{\Delta S_{AB}}{k_B} - \frac{\Delta E_{AB}}{k_B T}\right) \tag{4}$$

4.2 Interpretation of Entropic Parameters

Next, we turn to the interpretation of the entropy changes upon desorption $\Delta S_{d,i}$ obtained from our model. For a reversible adsorption-desorption process and a negligible activation energy of adsorption, Campbell and Sellers developed a model to relate the standard entropy of adsorption S_{ad}^0 of the adsorbed species to the prefactor of a TPD experiment ν_0 [4,5]. They find that the standard entropy of the transition state S_{TS}^0 is identical to the entropy of the molecules in the gas phase except for the entropy in the reaction coordinate, *i.e.*, for translation orthogonal to the surface. Thus, the transition state is missing one translational degree of freedom, which results in equation 5 for adsorption entropy [4,5].

$$S_{ad}^0 = S_g^0 - S_{g,1D-trans}^0 - k_B \ln\left(\frac{h\nu_0}{k_B T}\right) \tag{5}$$

In our model, the prefactors of desorption from sites A and B are given by equation 6.

$$\nu_{0,i} = \frac{k_B T}{h} \exp\left(\frac{\Delta S_{d,i}}{k_B}\right) \tag{6}$$

Insertion of our prefactors in equation 5 yields equation 7 for the adsorption entropy.

$$S_{ad,i}^0 = S_g^0 - S_{g,1D-trans}^0 - \Delta S_{d,i} \tag{7}$$

To calculate adsorption entropies from our prefactors, we also need the standard entropy and standard 1D-translational entropy of the gas phase. For the standard gas phase entropy we use values tabulated in literature [6] and $S^0_{g,1D-trans}$ is assumed to be one third of the total translational entropy in the gas phase $S^0_{g,trans}$ as recommended by Campbell and Sellers [5]. The standard translational gas phase entropy is given by the Sackur-Tetrode equation [7], where p is the pressure and $\Lambda = h/\sqrt{2\pi m k_B T}$ the thermal wave length.

$$S^0_{g,1D-trans} = \frac{1}{3}S^0_{g,trans} = \frac{1}{3}k_B\left[\ln\left(\frac{k_B T}{p\Lambda^2}\right) + \frac{5}{2}\right] \tag{4}$$

For water, we obtain adsorption entropies of $S^0_{ad,A}(T_{max,A}) = -0.4\ k_B$ and $S^0_{ad,B}(T_{max,B}) = 16.1\ k_B$ for sites A and B, respectively. This means that water molecules adsorbed on site A seem to lose all their entropy upon adsorption while water molecules adsorbed on site B have almost the same entropy as the transition state. Hence, we seemingly obtain the two limiting cases possible for the adsorption of water on calcite. As discussed in the main text, this could be due to our model not including molecule-molecule interactions.

4.3 Numerical Calculations

For the numerical calculations we use a similar procedure as explained in our previous publication [8] for the case of quasi-equilibrium layer exchange. Desorption curves for systems with two types of adsorption sites were calculated numerically based on equations 2 to 4. To this end, equation 1 was integrated as a differential equation of the total coverage θ with a fourth order Runge-Kutta algorithm. The site coverages θ_A and θ_B necessary for evaluation of the total desorption rate r_d according to equation 1 were calculated at each simulation step by solving the equation system consisting of equation 2 and the coverage balance $\theta = \theta_A + \theta_B$. Equations 3 and 4 were used to

describe the temperature dependence of the rate constants of desorption and the equilibrium constant of site exchange.

References

[1]   R. Zhang, A. Ludviksson, and C.T. Campbell, *Surf. Sci.* **1993**, 289, 1-9.

[2]   M. A. Henderson, *Surf. Sci.* **1996**, 355, 151-166.

[3]   M. Meier, J. Hulva, Z. Jakub, J. Pavelec, M. Setvin, R. Bliem, M. Schmid, U. Diebold, C. Franchini and G. S. Parkinson, *Proc. Natl. Acad. Sci.* **2018**, 115, E5642–E5650.

[4]   C. T. Campbell and J. R. V. Sellers, *J. Am. Chem. Soc.* **2012**, 134, 18109–18115.

[5]   C.T. Campbell and J. R. V. Sellers, *Chem. Rev.* **2013**, 113, 4106-4135.

[6]   To calculate gas phase entropies we use the "Shomate equation" available at the NIST Chemistry Webbook, http://webbook.nist.gov/chemistry/, accessed 24.11.2022.

[7]   H. Tetrode, *Annalen der Physik* **1912**, 343, 7.

[8]   T. Dickbreder, R. Bechstein, and A. Kühnle, *Phys. Chem. Chem. Phys.* **2021**, 23, 18314-18321.